Theoretical Study of the Competition between Intramolecular Hydrogen Bonds and Solvation in the Cys-Asn-Ser Tripeptide

Catalina Soriano-Correa,[†,‡] Francisco J. Olivares del Valle,[†] Aurora Muñoz-Losa,[†] Ignacio Fdez. Galván,[†] M. Elena Martín,[†] and Manuel A. Aguilar*[,†]

Química Física, Universidad de Extremadura, Avenida de Elvas, s/n 06071 Badajoz, Spain, and Laboratorio de Química Computacional, FES Zaragoza, Universidad Nacional Autónoma de México (UNAM), C.P. 09230 Iztapalapa, México, D.F., Mexico

Received: April 19, 2010

A study of the competition between intra- and intermolecular hydrogen bonds and its influence on the stability of the Cys-Asn-Ser tripeptide in aqueous solution was performed by using the averaged solvent electrostatic potential from molecular dynamics method (ASEP/MD). The model combines a DFT-B3LYP/6-311+G(d) quantum treatment in the description of the solute molecule with NVT molecular dynamics simulations in the description of the solvent. In gas phase, the most stable structure adopts a C5 conformation. Somewhat higher in energy are found the PP_{II} and C7eq structures. In solution, the stability order of the different conformers is reversed: the PP_{II} structure becomes the most stable, and the C5 structure is strongly destabilized. The conformational equilibrium is shifted toward conformations in which the intramolecular hydrogen bonds (IHB) have been substituted with intermolecular hydrogen bonds with the water molecules. The solvent stabilizes extended structures without IHBs that are not stable in vacuum. The effect of the protonation state on the conformational equilibrium was also analyzed.

I. Introduction

Small peptides have often served as model systems for the study of the conformational behavior of more complicated biomolecules both in vacuum and in solution.[1,2] Their smaller sizes permit systematic studies impossible to perform in larger peptides, at the same time, many of the structural motives of proteins are already present in these simplified models. One of the peptides that has received the most attention has been the alanine dipeptide (Ace-Ala-NMe, AD) molecule.[2−4] Several studies have evidenced that the conformational equilibrium of this molecule is modified by the presence of the solvent; thus, while in vacuum, the global minimum has a C7eq structure;[4g] in water solution, the most probable conformer has a polyproline-II (PP_{II}) type structure,[3a] although many other structures have also been identified. A similar behavior is expected in related peptides.

In an effort to gain insight on the solvent influence on the structure and stability of peptides, in this paper, we undertake the study of the electronic structure and the geometric parameters of the Cys-Asn-Ser (CNS) peptide. The backbone of this molecule (Figure 1) is identical to that of AD; however, both molecules differ in the nature of the side groups (in AD, the B, C, D side groups are replaced by methyl groups). The presence of these groups permits the CNS tripeptide to form several types of intramolecular hydrogen bonds (IHB) between atoms belonging to the side groups and the atoms that form the peptide bond, something that does not occur in AD. Because of this, the CNS−water system could serve as a simplified model for checking the possible competition between intra- and intermolecular hydrogen bonds and the effect that this competition has on the conformational equilibrium.

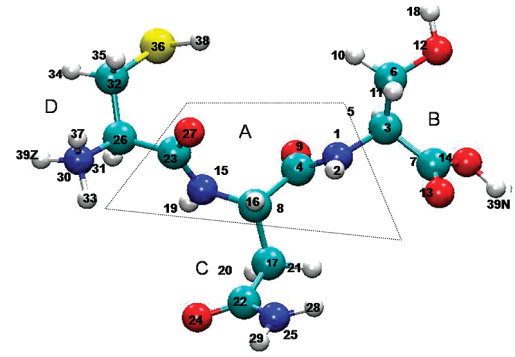

Figure 1. Atom numbering and labeling of the CNS tripeptide.

In addition, the CNS tripeptide also is of biological interest because of its anti-inflammatory activity in the amebiasis caused by the protozoon *Entamoeba histolytica*. This disease is currently a worldwide health problem.[5,6] In a previous work,[7] one of us carried out a detailed study at the Hartree−Fock and density functional theory (DFT) levels of the electronic structure, geometric parameters, physicochemical properties, and anti-inflammatory activity of three pentapeptides: (MLIF, Met-Gln-Cys-Asn-Ser; pMLIF, Met-Pro-Cys-Asn-Ser; and sMLIF, Gln-Cys-Met-Ser-Asn).[8] Further studies have evidenced that the critical functional fragment of these pentapeptides (MLIF and pMLIF) could correspond to the terminal tripeptide.[9] In vivo and in vitro studies on the anti-inflammatory activity of CNS concluded that it maintained 100% of the biological and anti-inflammatory properties of the MLIF. It is on this tripeptide that we have focused our attention.

Because of the great number of stable conformers, both in vacuum and in solution, that AD displays and the expected additional complexity resulting from the formation of IHBs in CNS, a detailed study of the full configurational space of CNS

* Corresponding author. E-mail: maguilar@unex.es.
† Universidad de Extremadura.
‡ Universidad Nacional Autónoma de México.

10.1021/jp1035162
Published on Web 06/22/2010

using ab initio quantum mechanics methods can be a prohibitively expensive task. Consequently, our aim has been more limited: taking as a starting point the structures that have been demonstrated to play an important role in the conformational equilibrium of AD, we study the effect that the competition between intra- and intermolecular hydrogen bonds has on the tripeptide structure. With this aim, we have identified some conformers that in gas phase display IHBs, and then we have proceeded to study their behaviors in water solution.

The competition between intra- and intermolecular hydrogen bonds is important due to the fact that IHBs determine the shape, properties, and functions of peptides and proteins.[10−12] For instance, measurements in globular proteins suggest a contribution to the conformational stability of between 1.0 and 2.2 kcal/mol per each additional IHB.[13,14] It is also well-known that the geometry, charge distribution and stability of IHBs can be affected by the presence of a solvent. Furthermore, when the solvent is a proton acceptor or donor, there is an additional factor to account for: the possible competition between intra- and intermolecular hydrogen bonds. This competition influences not only the structure and conformational equilibrium of peptides but also their intermolecular interactions in adsorption and molecular recognition processes. For instance, experimental results show that *p*-methylhydroxybenzoate and *p*-hydroxyacetophenone adsorb on acrylic ester with a 400-fold higher affinity than their ortho isomers, in which an intramolecular hydrogen bond is present.[15]

In our study, solvent effects were calculated with the averaged solvent electrostatic potential from molecular dynamics (ASEP/MD) method.[16] This method is especially adequate in the study of systems in which there is an interplay among solute polarization, solvent structure, and geometrical changes because it permits combining (1) a high-level ab initio description of the electronic structure of the solute, (2) the consideration of the mutual polarization of the solute and the solvent, (3) the location of minima on free energy surfaces, and (4) the calculation of free energy differences between different solute−solvent geometries.

The rest of the paper is organized as follows: Section II presents a short description of the main characteristics of the ASEP/MD method and of the way in which the free energy differences are calculated. Section III gives some computational details. The description of the most important conformers, their relative energies, and their properties are discussed in Section IV. Finally, Section V provides some conclusions.

II. Method

In the determination of the tripeptide electron structure and the solvent molecules' spatial distribution, we have used the ASEP/MD method developed in our laboratory.[16] ASEP/MD is a sequential QM/MM method that makes use of the mean field approximation;[17] that is, it introduces into the solute molecular Hamiltonian the perturbation generated by the solvent in an averaged way. The method combines quantum mechanics (QM) and molecular mechanics (MM) techniques with the particularity that full QM and MM calculations are alternated and not simultaneous. During the MD simulations, the intramolecular geometry and charge distribution of all the molecules are considered as fixed. From the resulting data, the average electrostatic potential generated by the solvent on the solute is obtained. This potential is introduced as a perturbation into the solute's quantum mechanical Hamiltonian, and by solving the associated Schrödinger equation, one gets a new charge distribution for the solute, which is used in the next MD simulation. The iterative process is repeated until the charge distribution of the solute and the solvent structure around it become mutually equilibrated.

As usual in QM/MM methods, the ASEP/MD Hamiltonian is partitioned into three terms[18]

$$\hat{H} = \hat{H}_{QM} + \hat{H}_{MM} + \hat{H}_{QM/MM} \tag{1}$$

corresponding to the quantum part, $\hat{H}_{QM}$; the classical part, $\hat{H}_{MM}$; and the interaction between them, $\hat{H}_{QM/MM}$. The quantum part comprises only the solute molecule. The classical part comprises all the solvent molecules.

The energy and wave function of the solvated solute molecule are obtained by solving the effective Schrödinger equation:

$$(\hat{H}_{QM} + \hat{H}_{QM/MM})|\Psi = E|\Psi\rangle \tag{2}$$

The interaction term, $\hat{H}_{QM/MM}$ takes the following form:

$$\hat{H}_{QM/MM} = \hat{H}^{elect}_{QM/MM} + \hat{H}^{vdw}_{QM/MM} \tag{3}$$

$$\hat{H}^{elect}_{QM/MM} = \int \mathrm{d}r\, \hat{\rho} \cdot \langle V_S(r;\rho)\rangle \tag{4}$$

where $\hat{\rho}$ is the solute charge density operator, and the brackets denote a statistical average. The term $\langle V_S(r;\rho)\rangle$, named ASEP, is the average electrostatic potential generated by the solvent at the position *r,* and it is obtained from MD calculations in which the solute molecule is represented by the charge distribution, ρ, and a geometry fixed during the simulation. The term $\hat{H}^{vdw}_{QM/MM}$ is the Halmiltonian for the van der Waals interaction, in general represented by a Lennard-Jones potential.

A few clarifications are relevant in this point. First, not all the configurations generated by the simulation are included in the ASEP calculation. We include only configurations separated by 0.05 ps. In this way, we decrease the statistical correlation between the selected configurations. Second, only the electrostatic term enters into the electron Hamiltonian. Other contributions to the solute−solvent interaction energy (repulsion and dispersion terms included in $\hat{H}^{vdw}_{QM/MM}$) are treated with empirical classical potentials, and since they depend only on the nuclear coordinates, they do not affect the solute electron wave function.

The in-solution peptide geometry was optimized using a technique described in a previous paper[19] and based on the use of the free energy gradient method.[20] The technique has been successfully applied to the geometry optimization of ground and excited states of molecules in solution. At each step of the optimization procedure, the mean value of the total force, *F*, and the Hessian, *H*, averaged over a representative set of solvent configurations are calculated as the sum of the solute and solvent contributions and are used to obtain a new geometry by using the rational function optimization method. The force and Hessian read[19]

$$F(r) = -\frac{\partial G(r)}{\partial r} = -\left\langle \frac{\partial V(r,X)}{\partial r} \right\rangle \approx -\frac{\partial \langle V(r,X)\rangle}{\partial r} \tag{5}$$

$$H(r, r') \approx \frac{\partial^2 \langle V(r, X) \rangle}{\partial r \, \partial r'} \quad (6)$$

where $G(r)$ is the free energy; $V(r,X)$ is a potential energy sum of intra- and intermolecular (solute−solvent) contributions; and the brackets denote a statistical average over the solvent configurations, X. Technical details about the practical application of this method and its relation with other methodologies can be found elsewhere.[19]

To determine the relative stability of the different conformers, the free energy difference was calculated. Here, we follow a dual-level methodology, in which the geometry and charges of the different conformers are obtained using quantum mechanical methods, but in which the interaction component of the free energy differences is calculated classically. The standard free energy difference between two conformers in solution is written as the sum of two terms,[21]

$$\Delta G = \Delta G_{\text{solute}} + \Delta G_{\text{int}} \quad (7)$$

where ΔG_{int} is the difference in the solute−solvent interaction free energy between the two QM states, and ΔG_{solute} is approximated as the ab initio difference between the two quantum-mechanical states (A and B) calculated using the in-vacuum solute molecular Hamiltonian, $\hat{H}_{\text{QM}}$ and the in solution wave functions:

$$\Delta G_{\text{solute}} = E^{\text{B}}_{\text{QM}} - E^{\text{A}}_{\text{QM}} = \langle \Psi^{\text{B}} | \hat{H}_{\text{QM}} | \Psi^{\text{B}} \rangle - \langle \Psi^{\text{A}} | \hat{H}_{\text{QM}} | \Psi^{\text{A}} \rangle \quad (8)$$

In this approximation, one neglects the difference in zero-point energy as well as entropy and thermal contributions to the solute QM free energy. The consideration of these terms does not introduce appreciable differences in the conformer stability in gas phase. We suppose that the same is valid in solution. Thermal and entropic contributions to the solute−solvent interaction energy are included in ΔG_{int} (see below).

The ΔG_{int} term was calculated using the free energy perturbation method.[22] The solute geometry was assumed to be rigid and a function of a perturbation parameter (λ), and the solvent was allowed to move freely. When $\lambda = 0$, the solute geometry and charges correspond to the initial state. When $\lambda = 1$, the charges and geometry are those of the final state. For intermediate values, a linear interpolation is applied. A value of $\Delta\lambda = 0.01$ was used. That means that a total of 101 separate molecular dynamics simulations were carried out to determine the free energy difference. To test the convergence of the calculation, the interaction free energies calculated forward and backward were compared.

III. Computational Details

The MD simulations were carried out using the program MOLDY.[23] The simulation contains one peptide molecule and 500 TIP3P[24] water molecules at fixed intramolecular geometry in a cubic box of 24.92 Å side. The atom numbering of the tripeptide is displayed in Figure 1. The solute parameters were obtained by combining Lennard-Jones interatomic interactions[25] with electrostatic interactions. Periodic boundary conditions were applied, and spherical cutoffs were used to truncate the peptide−water and water−water interactions at 9 Å. The electrostatic interaction was calculated with the Ewald method. The temperature was fixed at 298 K using the Nosé−Hoover[26] thermostat. Each simulation was run for 150 000 time steps, 50 000 for equilibration, and 100 000 for production. A time step of 0.5 fs was used. The final results were obtained by averaging the last five ASEP/MD cycles (250 ps).

The quantum calculations were performed at the DFT-B3LYP level of theory using the Gaussian98 package[27] of programs. The basis set used was 6-311+G(d). Atomic charges were calculated using the CHELPG method.[28]

Because of the presence in CNS of ionizable groups, we considered different protonation states in gas phase and in solution, so in gas phase, the neutral forms (not ionized) are more stable than the corresponding zwitterionic forms. In contrast, in solution, the neutral forms are hardly probable, and the protonation state will be determined by the pH. At physiological pH, the most stable form is the zwitterionic. Cationic forms become stable only at very acid pH (<2). Despite the lower biological relevance of these forms, we include them also in our study because they can enlighten the influence that the protonation state has on the conformational equilibrium. In the rest of the paper, we will be concerned mainly with the comparison between the gas phase neutral forms and in-solution zwitterionic forms, with occasional references to the protonated forms.

IV. Results and Discussion

Because of the similarity of the AD and CNS backbones, we take as a starting point of our study of the competition between intra- and intermolecular HBs those structures identified as key in the description of AD. The conformations of AD are usually specified by the values of the flexible backbone dihedral angles ϕ (C23−N15−C8−C4) and ψ (N15−C8−C4−N1). In gas phase, the global minimum of AD is believed to be a C7eq structure ($\phi \approx -83°$, $\psi \approx 73°$) which is stabilized by an IHB that involves the O and H of the two peptide bonds (O27 and H2). Somewhat higher in energy is found the C5 structure ($\phi \approx -161°$, $\psi \approx 155°$). This is quite an extended structure in which steric hindrance is minimized. Finally, although the PP_{II} structure ($\phi \approx -75°$, $\psi \approx 150°$) is not a minimum in gas phase, in solution it is the global minimum. When one passes to CNS, the behavior changes as a consequence of the formation of IHBs. In fact, the PP_{II} structure becomes also a minimum in gas phase.

The structure of CNS is characterized by the presence of two peptide bonds and different functional groups that can form several intra- and intermolecular HBs. We were especially interested in the study of the IHBs formed between the oxygen (O24) of the Asn side chain with the two hydrogens (H2 and H19) bonded to the nitrogens (N1 and N15) of the peptide bonds, which can provide stiffness to the main chain of the tripeptide, and between the SH (H38) group of the Cys residue and the carbonyl oxygen (O9) of the Asn residue involved in the peptide bond because, as we will show later, it could stabilize the PP_{II} structure. We named these IHBs HB1a (N1−H2−O24), HB1b (N15−H19−O24), and HB2 (S36−H38−O9), respectively. The spatial structure of the tripetipde CNS can be stabilized by other intramolecular hydrogen bonds. For instance, the C7eq structure is stabilized by the interaction between O27 and H2 (IHB3). Other conformers have been found in solution, but at such high energy that they are not expected to contribute significantly to the conformational equilibrium.

In our study, we have tried to analyze four points: (1) the relative stability of the different conformations as given by ΔG and its components, eq 7; (2) the structural changes occasioned by the solvation; (3) the variation of potential-fitted atomic charges with the conformation and the solvation; and finally,

TABLE 1: Angles (in degrees) and Relative Gas Phase Energies (in kcal/mol) of Different Neutral Minima of CNS and the Corresponding Zwitterionic Conformers Calculated at the Same Geometries[a]

conformer	ϕ	ψ	ΔE (neut)	ΔE (zwitt)	IHB
Vac-4 (C5)	−169.4	−177.0	0.0	0.0	IHB1a
Vac-3 (PP_{II})	−78.3	158.6	2.3	−6.6	IHB1a, IHB2
Vac-5 (C7eq)	−89.8	67.8	2.4	−5.1	IHB3
Vac-2 (PP_{II})	−53.6	133.3	3.3	−10.3	IHB1b, IHB2
Vac-1 (PP_{II})	−63.1	142.4	3.5	−7.8	IHB2

[a] The last column details the IHBs formed in each conformer.

(4) the correlation between the solvent structure around the solute and the conformational changes. To this end, we have divided the tripeptide structure into four regions, displayed in Figure 1. The A region corresponds to the basic skeleton of the molecule and includes the two peptide bonds. Regions B−D correspond to the side groups of the three amino acids. The strategy that we have followed has been to identify neutral structures with IHBs in gas phase and then study the behavior of the corresponding protonated and zwitterionic forms in water with the aim of determining if these IHBs are stable also in solution.

Gas Phase Results. We began our study by checking the relative stability in gas phase of several molecular conformations characterized by the presence of one or more intramolecular hydrogen bonds. The in-vacuum optimization was initiated from structures in which the ϕ and ψ angles take values close to those corresponding to the C7eq, C5, and PP_{II} structures in AD. Furthermore, to increase the configurational space covered, we systematically varied the C8−C17−C22−O24 torsion angle. The relative energy values in vacuum for five minima of the neutral tripeptide (named Vac-1−Vac-5) and their geometries are displayed in Table 1 and in Figures 2 and 3. Three of these conformers (Vac-1−Vac-3) display ϕ and ψ values close to those of the PP_{II} structure; they differ from each other in the orientation of the Asn side group (area C in Figure 1). Vac-4 and Vac-5 are related to C5 and C7eq structures of AD, respectively. The different structures were characterized as minima by frequency analysis.

In gas phase, the most stable conformer is Vac-4. This is a spatially extended conformation related to the C5 structure in AD and where HB1a is formed. This geometry also favors the interaction between O27 and H28; however, the bond distance between these atoms (2.40 Å) questions its IHB character. Somewhat higher in energy (∼2.3 kcal/mol) are Vac-3 and Vac-5. Vac-3 is a PP_{II} structure characterized by the presence of two IHBs: IHB1a and IHB2. Vac-5 corresponds to a C7eq structure that is stabilized by the formation of IHB3. Finally, at higher energies (∼3.4 kcal/mol) are found Vac-1 and Vac-2. The two conformers display structures close to PP_{II} but somewhat distorted. As was above indicated, the three PP_{II} structures differ in the orientation of the Asn side group (C group) that determines the presence or absence of IHB1. In this way, Vac-2 is characterized by the presence of IHB1b and Vac-3 by IHB1a, whereas in Vac-1 O24 is not involved in the

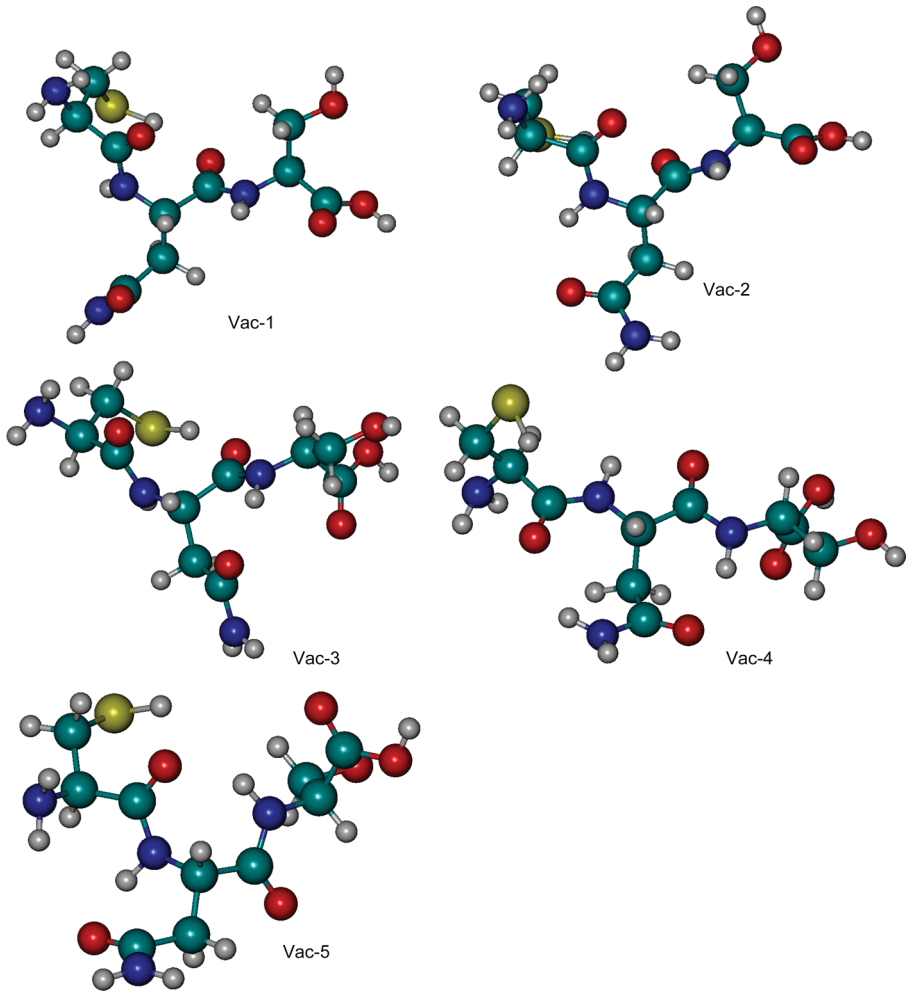

Figure 2. Minima structures in gas phase (neutral forms) of the CNS tripeptide.

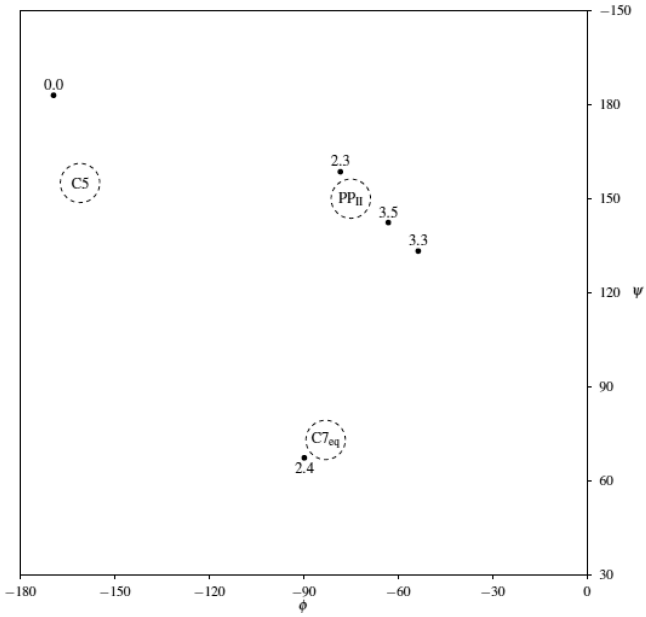

Figure 3. Free energy (in kcal/mol) of CNS in gas phase (neutral forms) as a function of the ϕ and ψ angles.

formation of any IHB. Note that O24 displays a larger preference to form IHB with H2 than with H19.

In Vac-3, the formation of the IHB generates a seven-atom ring, but in Vac-2, the ring has only six atoms. This permits a more favorable OHN angle (145.0°) in Vac-3 than in Vac-2 (125.1°). In the three PP_{II} conformers, HB2 is present. Since in AD the PP_{II} structure is not a minimum in gas phase, one can conclude that HB2 plays an important role in the stabilization of PP_{II} gas phase structures in CNS. It is also worth noting that, with respect to AD, there is an inversion of the relative stability between C5 and C7eq structures due to the formation in CNS of IHBs that are not present in AD: the C7eq structure is more stable in AD; in CNS, the C5 structure is preferred.

In sum, the presence of IHBs in CNS modifies the conformational equilibrium, stabilizing PP_{II} structures that are not stable in AD and reversing the stability order of C5 and C7eq conformers. For further comparison with in-solution results, Table 1 also displays the energy of the zwitterionic forms calculated at the geometry of the equivalent neutral forms. As a consequence of the charge separation in zwitterionic forms, the C5 structure is destabilized and the PP_{II} structures now become the most stable structures. As we will show below, this fact will modify the in solution relative stability order.

With respect to the structure of the side groups, region B can display a great variety of orientations, the internal energy hardly depending of this orientation. For instance, as the N2−H1−C3−C6 angle changes from 90° to 25°, the energy varies by only 0.1 kcal/mol. Because of the formation of HB2, the structure of region D is very similar in the three PP_{II} conformers. Finally, the orientation of region C with respect to the rest of the molecule is determined by the participation, or lack thereof, of O24 in the aforementioned IHBs. From Vac-1 to Vac-3, structures differ in the value of the C8−C17−C22−O24 angle that varies from −82° to 61°.

Figure 4 displays the charge distribution of the sections A−D defined in Figure 1 for different conformations. In all cases, there is a net flux of electrons from section B to section A, its magnitude being quite similar in all the conformers When the atomic charges are analyzed (data not shown in the figure), one finds that for most atoms there are only small variations from

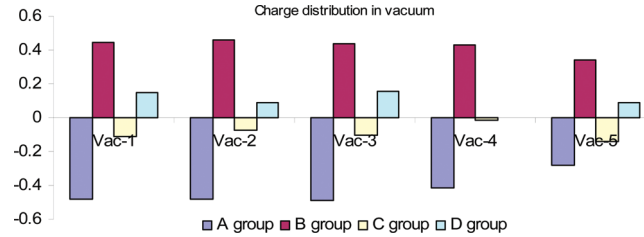

Figure 4. Potential fitted charges for the different conformers (neutral forms) in gas phase.

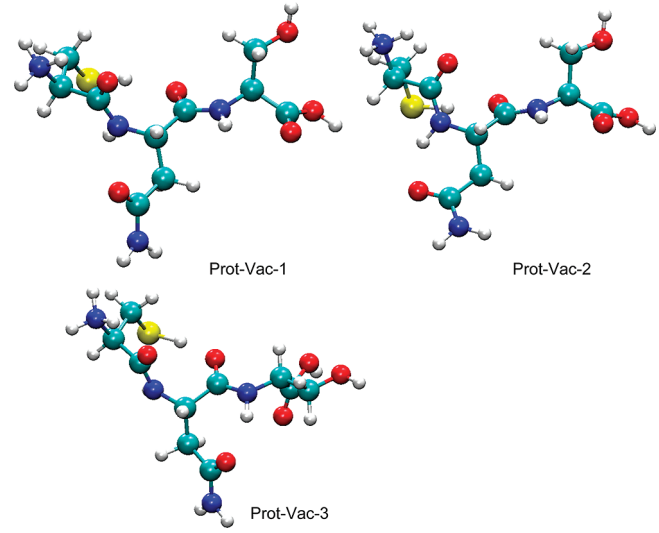

Figure 5. Minima structures in gas phase (protonated forms) of the CNS tripeptide.

TABLE 2: Angles (in degrees) and Relative Gas Phase Energies (in kcal/mol) of Different Minima of CNS (protonated forms)[a]

conformer	ϕ	ψ	ΔE	IHB
Prot−Vac-3 (PP_{II})	−74.5	165.6	0.0	IHB1a, IHB2
Prot−Vac-2 (PP_{II})	−58.7	151.7	0.3	IHB1b, IHB2
Prot−Vac-1 (PP_{II})	−85.8	163.6	2.0	IHB2

[a] The last column details the IHBs formed in each conformer.

one conformer to another. The standard deviation is lower that 0.1 *e* for 32 of the 39 atoms. In a reduced number of cases (N1, C3, C4, C8, C23, C26, and C30), there are important variations of the charge with the conformation. In this way, for instance, differences of 0.5 *e* between the charges on C4 in Vac-2 and Vac-6 are found. Although these results confirm the validity of using conformation-independent charges in molecular mechanics force fields for most atoms, they also evidence that in certain cases, this approximation fails, and it would yield wrong electrostatic interaction energies if the molecule were solvated. We will return on this point later.

Finally, and for further comparison with in solution calculations, we considered also the protonated versions of the three PP_{II} minima, (see Figure 5 and Table 2). Structures completely similar to the neutral ones were found. Although the stability order is the same as in the neutral forms, protonation slightly modifies the relative stability of the different conformers. The main change with respect to the neutral forms is that the free energy difference between Prot-Vac-3 and Prot-Vac-1 increases from 1.2 to 2.0 kcal/mol and between Prot-Vac-3 and Prot-Vac-2 decreases from 1.0 to 0.3 kcal/mol, now being difficult to conclude whether there is a neat preference for IHB1a or IHB1b. The two intramolecular hydrogen bonds, IHB1a and

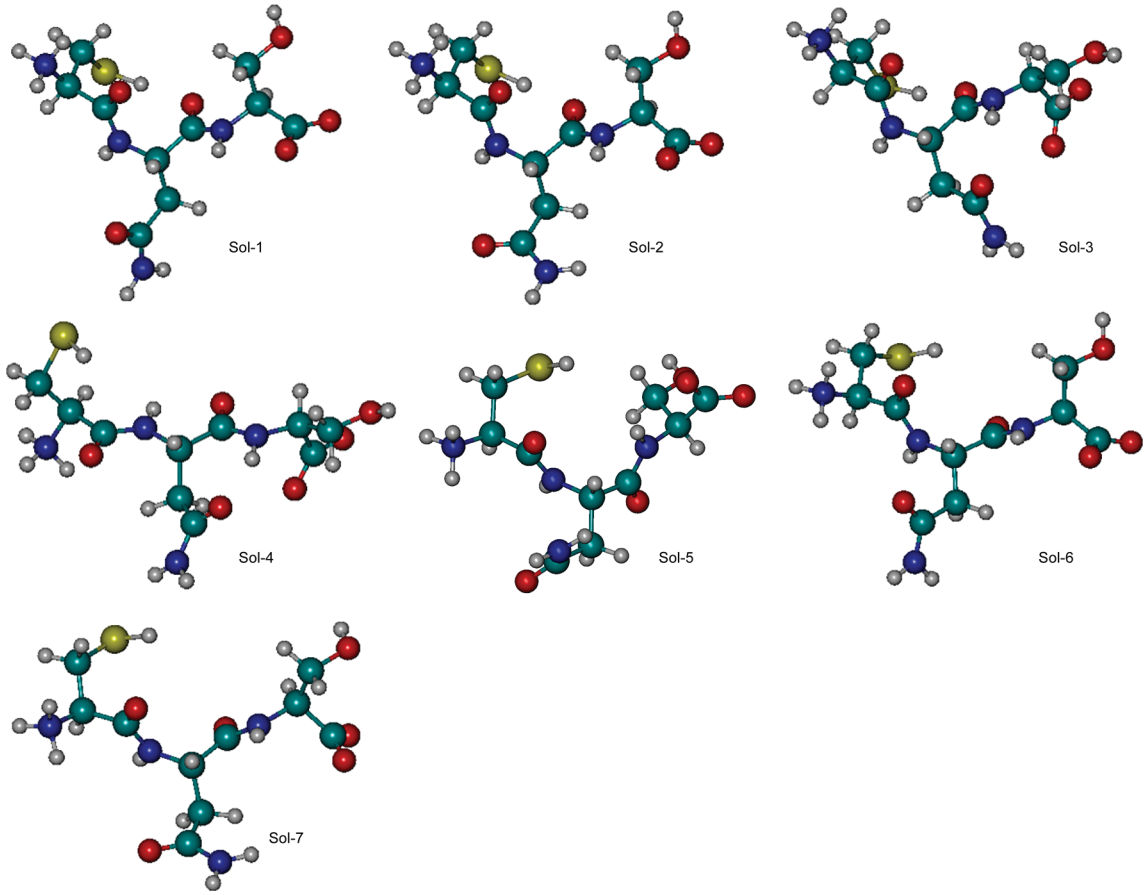

Figure 6. Minima structures in water solution (zwitterionic forms) of the CNS tripeptide.

TABLE 3: Angles (in degrees) and Relative in Solution Free Energies (in kcal/mol) of Different Minima of CNS (zwitterionic forms)[a]

conformer	ϕ	ψ	ΔG	IHB
Sol-6 (PP_{II})	−94.8	136.0	−5.7	
Sol-1 (PP_{II})	−61.8	149.4	−5.3	IHB2
Sol-5 (C7eq)	−117.4	92.8	−5.3	
Sol-7 (PP_{II})	−93.0	150.0	−2.8	
Sol-2 (PP_{II})	−60.1	147.5	−2.6	IHB2
Sol-3 (PP_{II})	−57.8	147.2	−0.2	IHB1a, IHB2
Sol-4 (C5)	−166.9	167.2	0.0	IHB1a

[a] The last column details the IHBs formed in each conformer.

IHB1b, seem to provide similar stability to the structure of the protonated tripeptide.

In-Solution Results. Figure 6 displays the structure of the most stable zwitterionic conformers in solution. In optimizing the geometries, we followed two different strategies. In the first one, the optimization started from the in vacuum optimized structures. In the second strategy, we used as initial geometries the same initial structures that were used in vacuum. In both cases, a proton was added to the Cys amino group, and a proton was removed from the terminal carbonyl group.

To facilitate the comparison between gas phase and in-solution results, we have tried to keep the same notation in both phases. For instance, Sol-1 is the structure obtained when Vac-1 is solvated, and so on. The values of the ϕ and ψ angles and the relative free energy of the different conformers are displayed in Table 3 and Figure 7. The first conclusion is that the solvent induces important changes both in the relative stability and in the structure of the conformers. Most IHBs are broken and transformed into intermolecular HBs with the water molecules

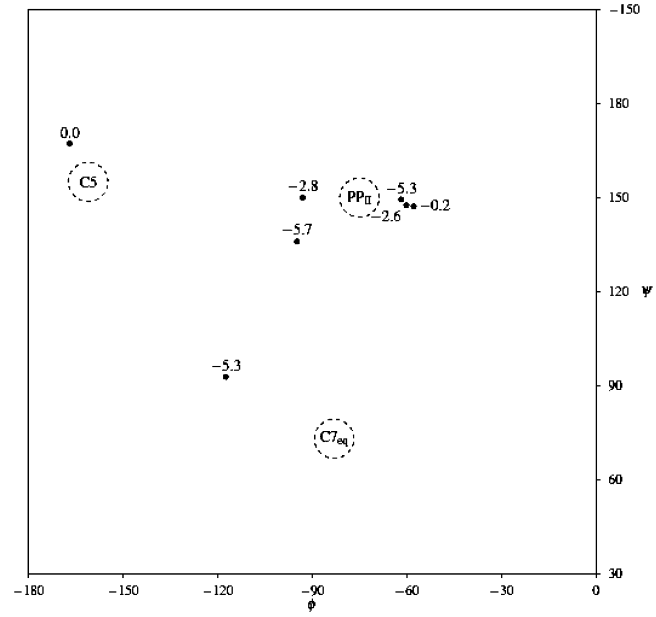

Figure 7. Free energy (in kcal/mol) of CNS in solution (zwitterionic forms) as a function of the ϕ and ψ angles.

during the solvation procedure. The solvent stabilizes structures without IHBs that are not stable in vacuum. Our results confirm previous studies about the relative stability of amino acids and peptides, in which it was found that some structures that do not exist in gas phase become stable in solution due to their ability to form strong intermolecular hydrogen bonds with water.[29]

TABLE 4: Free Energy Difference (relative to Sol-4) and Its Components, in kcal/mol, for the Minima of the Zwitterionic Forms in Solution

	ΔG_{solute}	ΔG_{int}	ΔG
Sol-6	−2.0	−3.6	−5.7
Sol-1	−11.0	5.7	−5.3
Sol-5	−3.7	−1.6	−5.3
Sol-7	0.7	−3.5	−2.8
Sol-2	−10.8	8.2	−2.6
Sol-3	−8.8	8.6	−0.2
Sol-4	0.0	0.0	0.0

TABLE 5: Angles (in degrees) and Relative in-Solution Free Energies (in kcal/mol) of Different PP_{II} Minima of CNS (protonated forms)[a]

conformer	ϕ	ψ	ΔG	IHB
Prot−Sol-1	−84.4	162.0	−2.9	IHB2
Prot−Sol-7	−86.2	141.5	−2.8	
Prot−Sol-6	−94.3	153.2	−2.7	
Prot−Sol-2	−57.2	150.3	−1.6	IHB1b, IHB2
Prot−Sol-3	−74.4	162.7	0.0	IHB1a, IHB2

[a] The last column details the IHBs formed in each conformer.

TABLE 6: Free Energy Difference (relative to Prot–Sol-3) and Its Components, in kcal/mol, for the Minima of the Protonated Forms in Solution

	ΔG_{solute}	ΔG_{int}	ΔG
Prot−Sol-1	3.8	−6.7	−2.9
Prot−Sol-7	20.0	−22.8	−2.8
Prot−Sol-6	15.9	−18.6	−2.7
Prot−Sol-2	0.8	−2.4	−1.6
Prot−Sol-3	0.0	0.0	0.0

From the seven minima displayed in Table 3, five of them (Sol-1, Sol-2, Sol-3, Sol-6, and Sol-7) have structures close to PP_{II}, whereas Sol-4 is a C5 structure. Finally, Sol-5 is a minimum obtained from the gas phase C7eq structure in which HB3 is broken and in which the structure has deformed to get a better exposition of the atoms of the peptide bonds to the solvent. The most stable structures are Sol-1, Sol-5, and Sol-6. In the three conformers, O24 forms an intermolecular HB with the water molecules, and Sol-1 is furthermore stabilized by IHB2. Higher in energy are placed the Sol-7 and Sol-2 conformers. Whereas Sol-7 does not display IHBs, Sol-2 is stabilized by IHB2. Sol-3 and Sol-4 are the least stable conformers, despite the presence of IHB1a in both of them.

From these results, several conclusions on the contribution of the IHBs to the stability are obtained: (1) In solution, the structures where O24 forms intermolecular hydrogen bonds with water molecules are strongly favored. Conformers in which IHB1a is present do not contribute in an appreciable way to the conformational equilibrium. Furthermore, we did not find any minimum with IHB1b. (2) From the five PP_{II} minima, in three of them, IHB2 is formed but not in the other two. The conformers in which HB2 is present are slightly less stable than the corresponding conformers in which IHB2 is not formed, but in general, differences are small. It is worth noting that in two of the PP_{II} minima, Sol-7 and Sol-6, IHB2 is not formed; therefore, the in-solution stability of the PP_{II} structure in this conformer must be associated with a larger solute−solvent interaction, a trend previously reported in AD. (3) In solution, the stability order is reversed with respect to the situation found in vacuum: the most stable structures in gas phase become the least stable ones in solution.

The study of the different contributions to the free energy, Table 4, permits us to clarify the origin of the inversion in the differential stability of the conformers when the system passes from vacuum to solution. ΔG is the sum of two contributions: the internal energy, ΔG_{solute}, and the solvation energy, ΔG_{int}. The internal energy follows the same trend already found in gas phase for the zwitterionic forms: a stabilization of the PP_{II} structures and a destabilization of C5. Regarding the solvation energy, it is more negative in those structures in which there is a larger exposition of the polar groups of the tripeptide to the water molecules; that is, in those structures in which the tripeptide adopts a conformation without IHBs (Sol-5, Sol-6, and Sol-7). The final stability order results from the interplay of internal energy and solvation, which, in turn, is in part determined by the competition between intra- and intermolecular HBs.

Similar results were obtained for the protonated form in solution (see Tables 5 and 6 and Figure 8). The three gas phase PP_{II} conformers originate five PP_{II} minima in solution; in three

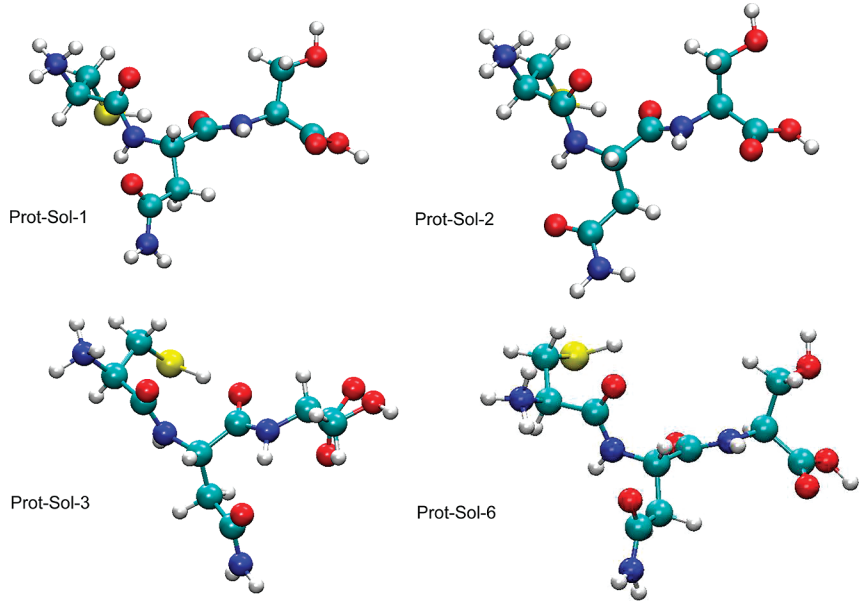

Figure 8. Minima structures in water solution (protonated forms) of the CNS tripeptide.

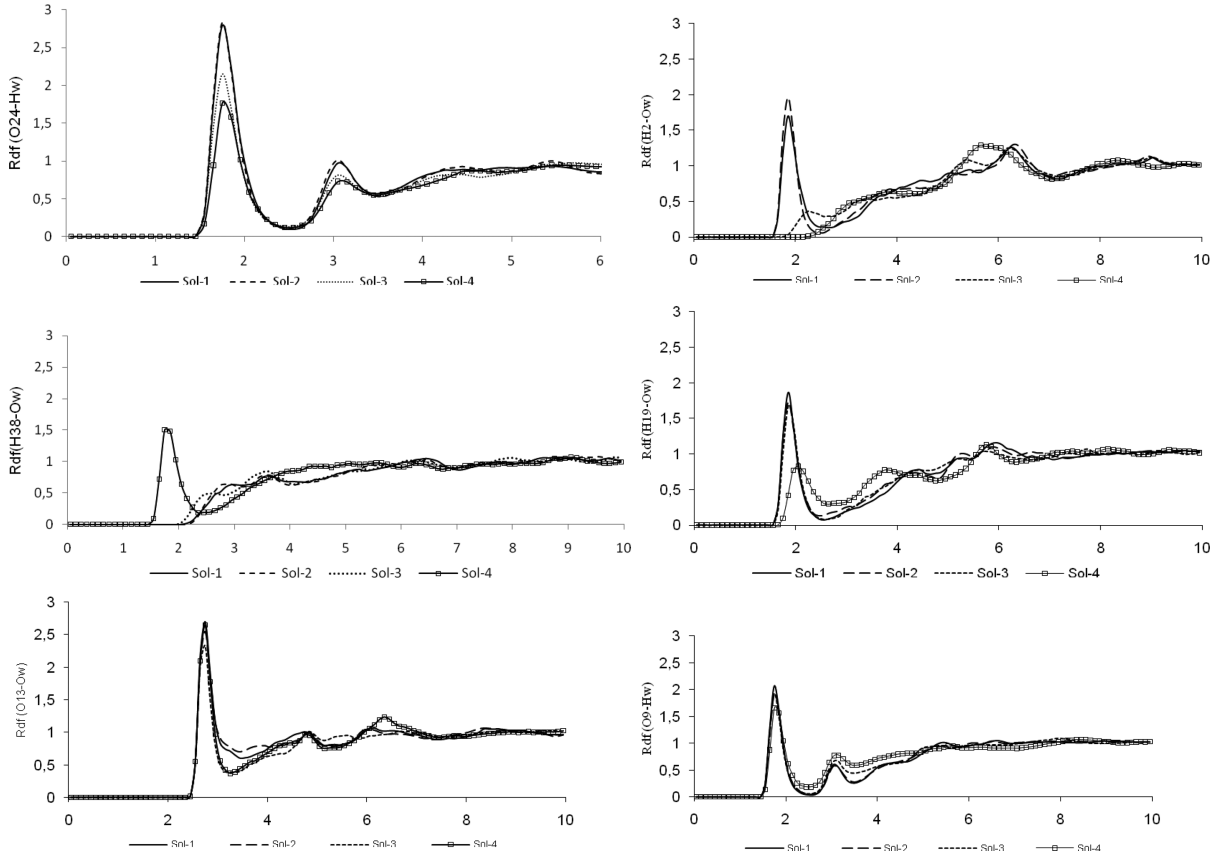

Figure 9. Radial distribution functions of some of the atoms implied in IHBs (zwitterionic forms).

of them, IHB2 is formed, but not in the other two. As occurred in the zwitterionic forms, the conformers in which IHB2 is formed are slightly less stable than the corresponding conformers in which IHB2 is not present. It is interesting to note that also in the protonated forms, there exists a strong negative correlation between the internal energy and the solvation energy: in general, the less stable the internal structure of the conformer, the greater the solvation energy. The relative stability order of protonated and zwitterionic forms is very similar; the only difference appears in the reverse order of Sol-1 and Sol-5. In any case, the energy differences between these two conformers is so small that it is difficult to reach a definitive conclusion. A fact to remark is that in protonated forms, the energy differences between the different conformers decrease with respect to the zwitterionic forms, passing from 5.7 to 2.9 kcal/mol. In sum, protonated and zwitterionic forms display a similar behavior in solution. Even if the protonation state does not modify the general trend found in the solvation of CNS, it can introduce small changes in the relative stability of the conformers by reducing the energy differences. However, in general, these changes are not enough to modify the relative stability order.

The study of the height and position of the radial distribution functions (rdf) peaks and of the coordination numbers also reflects the competition between intra- and intermolecular hydrogen bonds (see Figure 9). If one focuses the attention on the O24(CNS)−H(w) rdf, it is noted that the height of the rdfs decreases as one passes from a conformation with intermolecular HBs to another with intramolecular HBs. However, the more dramatic effect produced by the presence of IHB is displayed by the H2(CNS)−O(w) rdfs. Both Sol-1 and Sol-2 rdfs show well-defined peaks at 2 Å, their coordination numbers being close to 1. In contrast, in Sol-3 and Sol-4, there is a complete loss of the structure, evidencing the existence of an intramolecular hydrogen bond between O24 and H2.

A similar behavior can be noted in the H38(CNS)−O(w) rdfs, in which the effect of IHB2 is evidenced. Another interesting aspect is the analysis of the influence of the conformation on the rdfs of atoms not directly involved in IHBs. The main conclusion is that, in general, the rdfs of atoms of side groups (see, for instance, O13(CNS)−O(w) rdf) do not display appreciable changes from one conformer to other. Larger variations are found in atoms involved in the peptide bonds. Especially notable is the behavior of Sol-4, in which the height of the H19(CNS)−O(w) and O9(CNS)−H(w) rdf peaks decrease with respect to the other conformers. This fact joined to the presence of IHB1a that, as we have shown above, decreases the solvation of O24 can help to explain the low relative stability of this conformer in aqueous solution.

The data gathered in Table 7 permits us to analyze the solvent influence on the solute geometry. Solvation originates changes in the bond distances lower than 0.03 Å. The largest variations are found in the peptide bonds: O−C distances increase, and C−N distances decrease, and simultaneously, the planarity of the peptide bond increases slightly in solution. These behaviors are compatible with an increase in the stability of the charge-separated form of the peptide bond in water solution. There are also important variations in the bond distances of atoms involved in intermolecular hydrogen bonds with water, especially O24 and N30.

Finally, Figure 10 shows the variation of the in-solution charges with the conformation. Results are very similar to those obtained for the neutral conformers in gas phase. The main difference is that the variation of the charges between different conformations is smaller in solution than in vacuum. The largest variations ($\sim 0.25\ e$) are found in N1 and N13. These variations are clearly lower that those found in gas phase. The use of the same set of charges regardless of the conformation is more advisable in solution than in vacuum. To check whether the

TABLE 7: Selected Geometric Parameters

atoms	Sol-1	Sol-2	Sol-3	Sol-4	Sol-5	Sol-6	Sol-7	Vac-1	Vac-2	Vac-3	Vac-4	Vac-5
N_1H_2	1.021	1.022	1.013	1.018	1.013	1.021	1.022	1.011	1.011	1.016	1.020	1.019
$N_{15}H_{19}$	1.021	1.020	1.021	1.018	1.024	1.022	1.022	1.012	1.012	1.013	1.014	1.012
$N_{30}H_{37}$	1.036	1.036	1.036	1.036	1.036	1.036	1.037	1.017	1.017	1.017	1.016	1.016
C_4O_9	1.239	1.238	1.237	1.237	1.233	1.237	1.235	1.224	1.220	1.224	1.223	1.221
$C_{23}O_{27}$	1.230	1.232	1.231	1.234	1.229	1.234	1.233	1.224	1.230	1.221	1.235	1.232
$C_{22}O_{24}$	1.241	1.244	1.242	1.245	1.249	1.241	1.246	1.217	1.223	1.225	1.229	1.227
$S_{36}H_{38}$	1.354	1.354	1.353	1.358	1.362	1.360	1.359	1.355	1.354	1.355	1.352	1.351
N_1C_4	1.333	1.332	1.335	1.332	1.337	1.336	1.337	1.357	1.359	1.355	1.354	1.358
$N_{15}C_{23}$	1.338	1.337	1.339	1.332	1.343	1.335	1.338	1.364	1.353	1.370	1.352	1.359
$H_{38}O_9$	2.296	2.234	2.249			3.400	3.890	2.232	2.452	2.163		
$H_{33}O_{27}$	2.704	2.759	2.675	2.704	2.635	2.504	2.706	2.416	2.487	2.403	2.736	3.010
$O_{24}H_{19}$	3.301	3.046	4.707	4.956	3.766	3.645	3.717		2.122			2.170
$O_{24}H_2$	4.360	4.946	2.212	1.936	5.935	4.259	4.954			2.006	2.031	
$H_{33}O24$												2.788
$O_{27}H_2$												2.030
$C_4C_8C_{17}C_{22}$	166.840	154.754	74.562	93.818	178.020	165.472	146.505	168.852	−176.269	77.958	99.597	−176.885
$C_8C_{17}C_{22}O_{24}$	−14.753	66.754	15.053	−32.595	113.481	−18.647	73.952	−44.715	60.884	6.078	−81.971	62.892
$O_9C_4N_1H_2$	176.979	177.341	−170.029	−170.425	−179.158	35.465	−176.662	171.319	167.170	−168.480	−169.834	175.566
$O_{27}C_{23}N_{15}H_{19}$	−178.141	−177.966	−176.270	−107.757	−178.340	−177.415	−174.169	−163.736	174.639	−162.443	−171.846	168.029
$N_1C_4C_8N_{15}$	149.450	147.554	147.164	167.615	93.011	150.039	136.819	142.403	133.351	158.587	−177.034	67.781
$C_{23}N_{15}C_8C_4$	−61.760	−60.110	−57.810	−166.860	−117.335	−93.251	−94.822	−63.140	−53.644	−78.323	−169.412	−89.835

charge fluctuations have an appreciable effect on the solute−solvent interaction energies and, hence, on the conformational equilibrium, we recalculated the energy of the different conformers using the charges obtained for the others. Variations of the solute−solvent interaction energy comprised between 5% and 8% were found.

V. Conclusions

In this paper, we have tackled the study of solvent effects on the conformational stability of a tripeptide. In gas phase, it is found that the presence of IHBs in CNS modifies the conformational equilibrium with respect to AD, stabilizing PP_{II} structures that were not stable in AD and reversing the stability order of C5 and C7eq conformers. In solution, the solvent affects the conformational equilibrium in several ways: (1) modifying the number of intramolecular HBs, some of which can be replaced by intermolecular HBs with the water molecules; (2) shifting the conformational equilibrium by favoring those configurations (mainly with PP_{II} structures) with larger solute−solvent interaction energies; and (3) modifying the internal energy of the IHBs through changes in the geometry and charge distribution of the atoms.

There exists a strong trend to replace the IHBs in which O24 is involved by intermolecular HBs with the water molecules. In fact, structures in which IHB1b is present are not found in solution, and those structures with IHB1a are strongly destabilized. The same occurs with IHB3. This HB is responsible for the high stability of C7eq structures in both AD and CNS, and it is completely broken when we pass to solution. As a consequence of the transformation of neutral gas phase forms into in solution zwitterionic forms and the replacing of IHBs by intermolecular HBs, the stability order in solution is reversed with respect to the situation found in vacuum. The C5 structure that was the most stable in gas phase is strongly destabilized in solution. In contrast, PP_{II} structures (especially those with a lower number of IHBs) become stabilized. In general, there is a negative correlation between the internal and the solvation energies that, in turn, are a function of the number of IHBs.

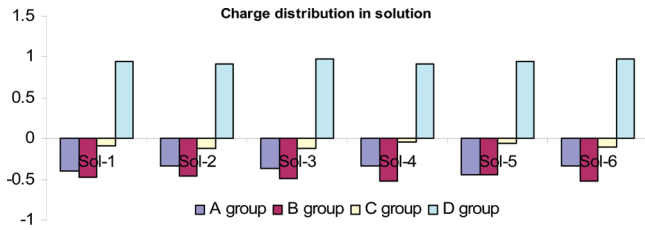

Figure 10. Potential fitted charges for the different conformers (zwitterionics forms) in solution.

With respect to IHB2, there is no clear trend. This bond is responsible for the stabilization of PP_{II} structures in gas phase but not in solution, in which the SH group does not display a clear preference between inter- and intramolecular hydrogen bonds. Structures in which O24 and SH form intermolecular hydrogen bonds with water molecules are more stable than those other structures in which these atoms are involved in the formation of IHBs. However, although the breaking of IHB2 provides an additional stability of only about 0.2−0.4 kcal/mol, the breaking of IHB1 seems to provide a stabilization of several kilocalories per mole.

From a comparison of the zwitterionic and protonated minima, it was concluded that the protonation state does not introduce important changes in the in-solution relative stability order. Its main effect is to reduce the energy difference among the different conformers.

Acknowledgment. This work was supported by the CTQ2008-06224 Project from the Ministerio de Educación y Ciencia of Spain and the PRI08A056 Project from the Consejería de Economía, Comercio e Innovación of the Junta de Extremadura. C.S.C. acknowledges a fellowship from the Junta de Extremadura.

Supporting Information Available: Cartesian coordinates of all the structures discussed in the text. This material is available free of charge via the Internet at http://pubs.acs.org.

References and Notes

(1) Brooks, C.; Case, D. A. *Chem. Rev.* **1993**, *93*, 2487.
(2) Pettitt, B. M.; Karplus, M. *J. Phys. Chem.* **1988**, *92*, 3994.
(3) (a) Poon, C. D.; Samulski, E. T.; Weise, C. F.; Weisshaar, J. C. *J. Am. Chem. Soc.* **2000**, *122*, 5642. (b) Kim, Y. S.; Wang, J.; Hochstrasser, R. M. *J. Phys. Chem. B* **2005**, *109*, 7511. (c) Kang, Y. K. *J. Phys. Chem. B* **2006**, *110*, 21338. (d) Graf, J.; Nguyen, P. H.; Stock, G.; Schwalbe, H. *J. Am. Chem. Soc.* **2007**, *129*, 1179.
(4) (a) Tobias, D. J.; Brooks, C. L. *J. Chem. Phys.* **1992**, *96*, 3864. (b) Marrone, T. J.; Gilson, M. K.; McCammon, J. A. *J. Phys. Chem.* **1996**, *100*, 1439. (c) Beachy, M. D.; Chasman, D.; Murphy, R. B.; Halgren, T. A.; Friesner, R. A. *J. Am. Chem. Soc.* **1997**, *119*, 5908. (d) Smith, P. E. *J. Chem. Phys.* **1999**, *111*, 5568. (e) Kalko, S. G.; Guardia, E.; Padró, J. A. *J. Phys.*

Chem. B **1999**, *103*, 3935. (f) Cui, Q.; Elstner, M.; Kaxiras, E.; Frauenheim, T.; Karplus, M. *J. Phys. Chem. B* **2001**, *105*, 569. (g) Vargas, R.; Garza, J.; Hay, B. P.; Dixon, D. A. *J. Phys. Chem. A* **2002**, *106*, 3213. (h) Seabra, G. M.; Walter, R. C.; Roitberg, A. E. in *Solvation effects on molecules and biomolecules*; Canuto, S., Ed.; Springer Science: Berlin, 2008; p 507.

(5) WHO. *The World Health Report*; 1995-Bridging the GapsWorld Health Forum, 1995; Vol. 16, pp 377−385.

(6) Pérez-Tamayo, R. *Amebiasis*; Elsevier: Amsterdam, 1986.

(7) Soriano-Correa, C.; Sánchez-Ruiz, J. F.; Rico-Rosillo, G.; Giménez-Scherer, J. A.; Velázquez-Rodríguez, J.; Kretschmer-Schmid, R. *J. Mol. Struct. (Theochem)* **2006**, *769*, 91.

(8) Rico, G.; Leandro, E.; Rojas, S.; Giménez, J. A.; Kretschmer, R. *Parasitology* **2003**, *90*, 264.

(9) Morales, M. E.; Silva, R.; Soriano-Correa, C.; Giménez-Scherer, J. A.; Rojas, S.; Blanco-Favela, F.; Rico-Rosillo, G. *Mol. Biochem. Parasitol.* **2008**, *158*, 46.

(10) Makarov, V.; Pettitt, B. M.; Feig, M. *Acc. Chem. Res.* **2002**, *35*, 376.

(11) Kaur, D.; Kohli, R. *Int. J. Quantum Chem.* **2008**, *108*, 119.

(12) Schmitt, M.; Böhm, M.; Ratzer, C.; Vu, C.; Kalkman, I.; Meerts, W. L. *J. Am. Chem. Soc.* **2005**, *127*, 10356.

(13) Takano, K.; Yamagata, Y.; Funahashi, J.; Hioki, Y.; Kuramitsu, S.; Yutani, K. *Biochem.* **1999**, *38*, 12698.

(14) Myers, J. K.; Pace, C. N. *Biophys. J.* **1996**, *71*, 2033.

(15) Glemza, A. J.; Mardis, K. L.; Chaudhry, A. A.; Gilson, M. K.; Payne, G. F. *Ind. Eng. Chem. Res.* **2000**, *39*, 463.

(16) Fdez. Galván, I.; Sánchez, M. L.; Martín, M. E.; Olivares del Valle, F. J.; Aguilar, M. A. *Comput. Phys. Commun.* **2003**, *155*, 244.

(17) Sánchez, M. L.; Martín, M. E.; Fdez. Galván, I.; Olivares del Valle, F. J.; Aguilar, M. A. *J. Phys. Chem. B* **2002**, *106*, 4813.

(18) (a) Warshel, A.; Levitt, M. *J. Mol. Biol.* **1976**, *103*, 227. (b) Field, M. J.; Bash, P. A.; Karplus, M. *J. Comput. Chem.* **1990**, *11*, 700. (c) Luzhkov, V.; Warshel, A. *J. Comput. Chem.* **1992**, *13*, 199. (d) Gao, J. *J. Phys. Chem.* **1992**, *96*, 537. (e) Vasilyev, V. V.; Bliznyuk, A. A.; Voityuk, A. A. *Int. J. Quantum Chem.* **1992**, *44*, 897. (f) Théry, V.; Rinaldi, D.; Rivail, J.-L.; Maigret, B.; Ferenczy, G. G. *J. Comput. Chem.* **1994**, *15*, 269. (g) Thompson, M. A.; Glendening, E. D.; Feller, D. *J. Phys. Chem.* **1994**, *98*, 10465.

(19) (a) Fdez. Galván, I.; Sánchez, M. L.; Martín, M. E.; Olivares del Valle, F. J.; Aguilar, M. A. *J. Chem. Phys.* **2003**, *118*, 255. (b) Yamamoto, Y. *J. Phys. Chem.* **2008**, *129*, 244104.

(20) (a) Okuyama-Yoshida, N.; Nagaoka, M.; Yamabe, T. *Int. J. Quantum Chem.* **1998**, *70*, 95. (b) Okuyama-Yoshida, N.; Kataoka, K.; Nagaoka, M.; Yamabe, T. *J. Chem. Phys.* **2000**, *113*, 3519. (c) Hirao, H.; Nagae, Y.; Nagaoka, M. *Chem. Phys. Lett.* **2001**, *348*, 350.

(21) Muñoz Losa, A.; Fdez. Galván, I.; Martín, M. E.; Aguilar, M. A. *J. Phys. Chem. B* **2006**, *110*, 18064.

(22) (a) Kollman, P. A. *Chem. Rev.* **1993**, *93*, 2395. (b) Mark, A. E. In *Encyclopedia of Computational Chemistry*; Schleyer, P. v. R., Allinger, N. L., Clark, T., Gasteiger, J., Kollman, P. A., Schaefer, H. F., III, Schreiner, P. R., Eds.; Vol. 2. Wiley and Sons: Chichester, 1998, p 1070.

(23) Refson, K. *Comput. Phys. Commun.* **2000**, *126*, 310.

(24) Jorgensen, W. L.; Chandrasekhar, J.; Madura, J. D.; Impey, R. W.; Klein, M. L. *J. Chem. Phys.* **1983**, *79*, 926.

(25) Cornell, W. D.; Cieplack, P.; Bayly, C. I.; Groud, K. M.; Fergurson, D. M.; Spellmeyer, D. C.; Fox, T.; Cladwell, J. W.; Kollman, P. A. *J. Am. Chem. Soc.* **1995**, *117*, 5179.

(26) Hoover, W. G. *Phys. Rev. A* **1985**, *31*, 1695.

(27) Frisch, M. J. ; Trucks, G. W.; Schlegel, H. B.; Scuseria, G. E.; Robb, M. A.; Cheeseman, J. R.; Zakrzewski, V. G.; Montgomery, J. A., Jr.; Stratmann, R. E.; Burant, J. C.; Dapprich, S.; Millam, J. M.; Daniels, A. D.; Kudin, K. N.; Strain, M. C.; Farkas, O.; Tomasi, J.; Barone, V.; Cossi, M.; Cammi, R.; Mennucci, B.; Pomelli, C.; Adamo, C.; Clifford, S.; Ochterski, J.; Petersson, G. A.; Ayala, P. Y.; Cui, Q.; Morokuma, K.; Malick, D. K.; Rabuck, A. D.; Raghavachari, K.; Foresman, J. B.; Cioslowski, J.; Ortiz, J. V.; Baboul, A. G.; Stefanov, B. B.; Liu, G.; Liashenko, A.; Piskorz, P.; Komaromi, I.; Gomperts, R.; Martin, R. L.; Fox, D. J.; Keith, T.; Al-Laham, M. A.; Peng, C. Y.; Nanayakkara, A.; Gonzalez, C.; Challacombe, M.; Gill, P. M. W.; Johnson, B.; Chen, W.; Wong, M. W.; Andres, J. L.; Gonzalez, C.; Head-Gordon, M.; Replogle, E. S.; Pople, J. A. *Gaussian98*; Gaussian, Inc.: Pittsburgh PA, 1998.

(28) (a) Chirlian, L. E.; Francl, M. M. *J. Comput. Chem.* **1987**, *8*, 894. (b) Breneman, C. M.; Wiberg, K. B. *J. Comput. Chem.* **1990**, *11*, 316.

(29) Cui, Q. *J. Chem. Phys.* **2002**, *117*, 4720.

JP1035162